High-efficiency virtual cathode oscillator with photonic crystal

Nikita S. Frolov, Semen A. Kurkin, Alexey A. Koronovskii, Alexander E. Hramov, and Alexey O. Rak

Citation: Appl. Phys. Lett. **113**, 023503 (2018); doi: 10.1063/1.5038277
View online: https://doi.org/10.1063/1.5038277
View Table of Contents: http://aip.scitation.org/toc/apl/113/2
Published by the American Institute of Physics

High-efficiency virtual cathode oscillator with photonic crystal

Nikita S. Frolov,[1,2] Semen A. Kurkin,[1,2,a)] Alexey A. Koronovskii,[1,2] Alexander E. Hramov,[1,2] and Alexey O. Rak[3]
[1]*Yuri Gagarin State Technical University of Saratov, 410054 Saratov, Russia*
[2]*Saratov State University, 410012 Saratov, Russia*
[3]*Belarusian State University of Informatics and Radioelectronics, 220013 Minsk, Belarus*

(Received 2 May 2018; accepted 3 July 2018; published online 12 July 2018)

We study the properties of microwave generation in a virtual cathode oscillator with a photonic crystal composed of metal grids. Our simulation results show the high efficiency of photonic crystal structure utilization in comparison with the standard scheme of an axial virtual cathode oscillator: operation efficiency reaches 20% at the optimal parameters. The obtained results demonstrate that the virtual cathode oscillator with a photonic crystal can be considered as a prospective high-power microwave source where the vircator operation mechanism and photonic crystal properties complement each other to produce high-power electromagnetic radiation. *Published by AIP Publishing.*
https://doi.org/10.1063/1.5038277

High-power microwave (HPM) sources are applied in a wide range of challenging tasks in prospective areas of science and technology. Many HPM devices are closely related to fields of modern science such as acceleration of ions, plasma heating, and thermonuclear fusion. Along with pure fundamental science, HPM sources are of strong commercial interest (radar and communications, power beaming, space applications, etc.).[1–7]

There is a class of HPM devices, which excite particular interest of the scientific community and whose operation is based on the formation and oscillations of a virtual cathode (VC)—high-density space-charge cloud in an electron beam.[8–11] Due to mentioned space-charge phenomena, this class of HPM devices is called virtual cathode oscillators (VCOs) or vircators.[7,12–16] Vircators are known to be a rather simple way to extract electromagnetic energy from relativistic electron beams (REBs) and to generate microwaves, providing high-power radiation up to a gigawatt output peak power level, or to amplify powerful microwave signals.[16–22]

Along with advantages of VCOs such as high output power, construction simplicity, and capability to operate without application of the external magnetic field, one of the weakest points of vircators is low generation efficiency (0.1%–10%).[7,14,23–25] In basic VCO configurations, this issue is related to low efficiency of microwave output systems or poor bunching of electrons in the VC area.[7,13,26,27] Various modifications of standard vircator design have been proposed and investigated to improve microwave generation efficiency.[15,19,28–32] In our opinion, one of the most interesting approaches to enhance vircator characteristics has been proposed in the early 1990s in the experimental work by Gadetskii *et al.*[33] In this work, they have suggested the idea of the hybrid vircator and backward-wave oscillator (vircator-BWO) device. They have succeeded in the generation efficiency increase owing to creating additional electromagnetic feedback with VC by means of backward wave excitation in this device.

We assume that in this context, it is more perspective to use a photonic crystal (PC) as a slow-wave or output structure. Many recent studies, both theoretical and experimental, show attractive properties of these structures, namely their capacity to concentrate electromagnetic energy and to direct their flow.[34–38] The idea to combine the classical configuration of the axial vircator with the PC system has been stated by Baryshevsky in his work.[39] The authors suggested that the diffraction properties of PC and its high interaction impedance provide an additional generation mechanism in such a system. However, systematic studies of microwave generation processes and radiation characteristics in this system have not been carried out yet. Detailed investigations of this issue may provide effective solution to the mentioned problem of the VCO efficiency increase. So, current work is devoted to numerical investigation of the prospective VCO scheme with the PC output structure in the framework of 3D fully electromagnetic particle-in-cell (PIC) simulation.

Let us describe the design and numerical simulation details of the proposed VCO with PC. The schematic representation of the microwave device under study is presented in Fig. 1(a). According to this illustration, the vircator system with PC consists of a cylindrical drift tube (marked "1"), REB injector (marked "2"), focused REB (marked "3"), and PC foil grid structure (marked "4"). We set open boundary conditions at the right end of the drift tube to model electromagnetic energy output. The boundary conditions at the drift tube walls conform to perfect electric conductor (PEC) conditions. The inset in Fig. 1(a) shows the detailed view of one period of the PC structure. Here, the longitudinal axis is defined by the z letter and corresponds to the REB propagation direction. As it is seen from the figure, the structure of the PC represents a number of metal foil stripes located periodically in longitudinal and transverse directions to the beam propagation. So, this photonic crystal has two spatial periods: dz—in the longitudinal direction and dy—in the transverse direction. We should note that PC metal strips are electrically connected to the wall of drift tube to avoid their charging by the drifting REB. It is important to note that the

a)Electronic mail: kurkinsa@gmail.com

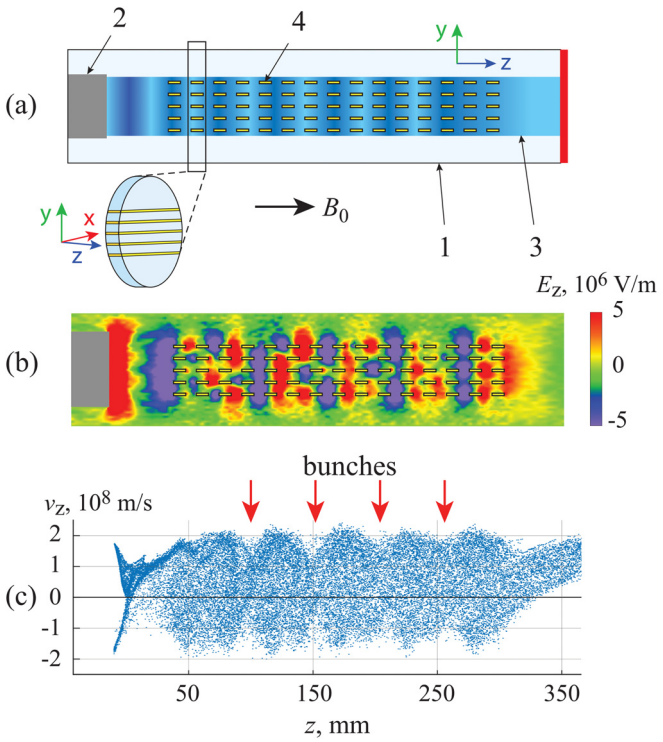

FIG. 1. (a) The schematic representation of the virtual cathode oscillator with PC. 1—cylindrical drift tube; 2—REB injector; 3—focused REB (color intensity is proportional to space charge density and demonstrates the formation of electron bunches); 4—microwave PC foil grid structure. The highlighted red surface at the right end of the drift tube is considered as open boundary. The inset shows the structure of one period of PC. (b) Cross-section of longitudinal component of electric field E_z at $x = 0$ and $t = 30$ ns that illustrates the excitation and propagation of electromagnetic waves in the periodic PC structure. (c) The phase portrait of the REB traveling through the drift tube with PC at $t = 30$ ns; beam current $I_0 = 2.75$ kA. Red arrows show the positions of bunches formed in the REB under the interaction with the induced electromagnetic wave in the PC.

application of the external magnetic field is necessary for efficient vircator operation. In this case, REB focusing increases the efficiency of the interaction between REB and PC.

We have chosen geometric parameters of the photonic crystal according to the work:[40] injector radius—35 mm, drift tube radius—45 mm, drift tube length—630 mm, distance between the injector and the photonic crystal—40 mm, PC spatial period along the y axis—9.5 mm, number of PC metal stripes along the y axis—5, metal stripe length along the z axis—10 mm, metal stripe thickness—0.1 mm, PC spatial period along the z axis—18 mm, and number of PC periods along the z axis—15. The maximum value of the applied magnetic field at the beam axis was 2 T. The initial potential of the beam was fixed during the simulations and equal to $U_0 = 120$ kV.

The main idea of PC application in the axial vircator scheme is an improvement of its microwave generation efficiency owing to the principal advantages of PC. The first of them is a possibility of effectively guiding the electromagnetic energy flow induced by the VC oscillations. The second is a realization of the additional generation mechanism related to the interaction between the drifting part of REB, which passes the potential barrier of VC, and PC eigenmodes. In this case, the part of REB pre-modulated by VC oscillations pierces PC and excites intensive electromagnetic waves [Fig. 1(b)]. The latter contributes to the efficiency gain due to the involvement of that part of the REB, which is out-of-use in the traditional vircator scheme. Moreover, Fig. 1(b) supplemented by Fig. 1(c) shows that the interaction between REB and PC is a self-consistent process, since longitudinal E_z waves are induced by REB trap beam particles and create bunches. This increases the efficiency of energy exchange between REB and electromagnetic field.

The characteristic feature of the PC structure is its dispersion diagram. It is known that in some frequency ranges, the dispersion curves of PC form bands for electromagnetic wave propagation, while in certain frequency ranges, there are bandgaps, where the wave propagation is impossible.[34,35] Figure 2 shows the band diagram of the considered PC calculated via the finite-difference method. The bold red line here corresponds to the undisturbed drifting REB with an energy of 120 keV and is defined as $f(k) = v_b k/2\pi$, where v_b is the beam drift velocity. It is obvious that such REB piercing of the PC will excite electromagnetic waves in certain frequency ranges which are highlighted in blue in Fig. 2. However, the REB excites most effectively the PC fundamental mode (see white point in Fig. 2), since the maximum of the electric field z-component of this mode is located at the REB propagation axis, which provides high beam-wave interaction impedance. Excitation of the fundamental mode of PC results in emergence of spectral components in corresponding frequency range I [for example, see Fig. 3(a)]. One can clearly see that electromagnetic field oscillations induced in area I are characterized by low intensity and rather low frequency (about 1.67 GHz), even from the viewpoint of the microwave range.

However, in this context, a combination of the vircator operation mechanism and PC dispersion properties appears very useful for effective operation in areas II and III, since the VC oscillation frequency lies in the range of PC high-

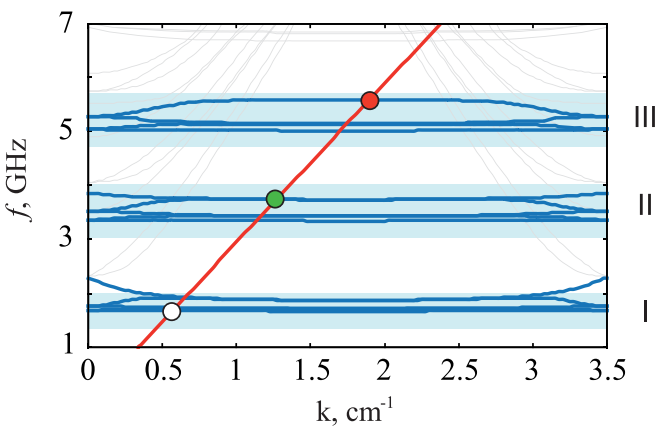

FIG. 2. Numerically obtained dispersion characteristics of the PC modes in the considered vircator system. Bold blue curves represent the dispersion characteristics of PC dominant modes and thin gray lines represent the rest ones. The red straight line corresponds to the dispersion characteristic of the REB with an initial energy of 120 keV. The most significant intersections of the REB and PC dispersion characteristics are marked with *white*, *green*, and *red* points. We note that the *white point* determines the excitation of the fundamental PC eigenmode; *green* and *red points*—excitation of the high-order PC eigenmodes at $I_0 = 2.5$ kA. Three areas of dispersion curves intersected by the beam line are highlighted with blue squares and marked as I, II, and III.

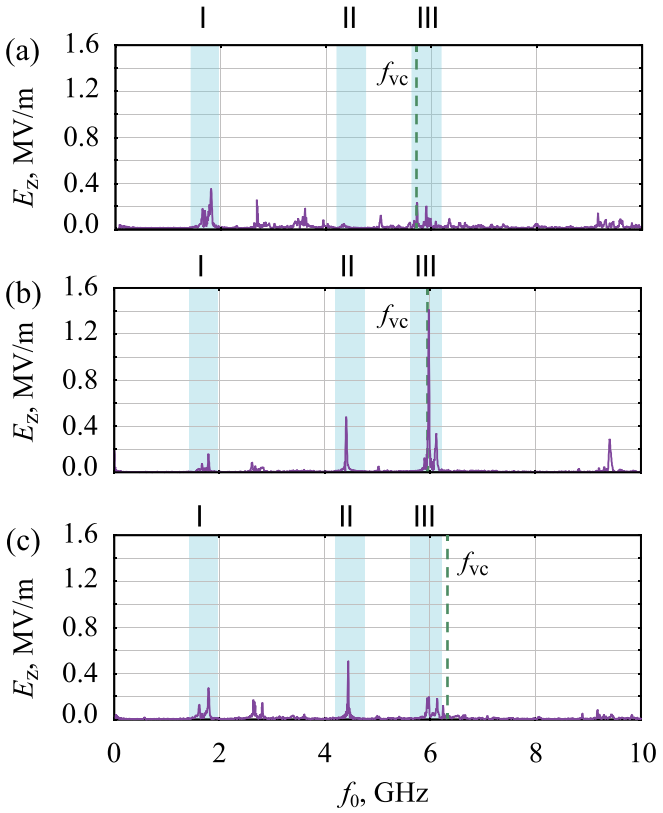

FIG. 3. The evolution of electric field oscillation Fourier-spectrum under the variation of the beam current I_0. The spectrum in (a) corresponds to the weak interaction between the beam and the photonic crystal at $I_0 = 2.0$ kA. The spectrum in (b) reflects the effective excitation of the photonic crystal eigenwave in area III by both virtual cathode oscillations and the modulated passing beam at $I_0 = 2.75$ kA. The spectrum in (c) shows the absence of the interaction between virtual cathode oscillations and the photonic crystal due to $f_{vc} > f_{III}$; $I_0 = 3.25$ kA. The *green* dashed line shows the position of virtual cathode oscillation frequency f_{vc} corresponding to I_0 at each plot. The oscillations of electric field longitudinal component E_z were recorded near the open boundary.

order bands. In this case, the part of REB passing through the VC potential barrier is obviously modulated at the frequency of VC oscillations, f_{vc}. As f_{vc} is easily controlled by the value of beam current, I_0, it gives an opportunity to realize the resonant excitation of photonic crystal high-order eigenmodes by the density modulated REB. From the viewpoint of increasing the VCO efficiency, it is more important to excite electromagnetic waves in the PC characterized by a negative group velocity: $\partial f/\partial k < 0$.

Let us illustrate the described mechanism by means of consideration of E_z Fourier-spectrum evolution under the variation of the initial beam current I_0 (see Fig. 3). First of all, it is notable that the low-frequency spectral component at $f = 1.67$ GHz corresponding to the fundamental eigenmode of the photonic crystal appears in the presented Fourier-spectra regardless of the value of I_0. Amplitude of this spectral component does not depend on I_0 noticeably. It means that excitation of the fundamental mode in the system is independent of processes of virtual cathode oscillations and modulation frequency of the transmitted beam; it is only determined by passing of the beam through the peak of electric field distribution of the photonic crystal fundamental eigenmode.

As one can see from Fig. 3(a) at $I_0 = 2.0$ kA, the REB with VC excites low-intensity waves in areas I, II, and III of the PC because VC oscillation frequency $f_{vc} = 5.53$ GHz, which determines the modulation frequency of the transmitted beam, lies in the bandgap of the PC, and does not match with any of the high-order PC dispersion curves. When $I_0 = 2.75$ kA and $f_{vc} \approx 5.95$ GHz is close to one of the dispersion curves (red point in Fig. 2), a sharp increase in amplitude of the spectral component corresponding to the VC oscillation frequency is observed [Fig. 3(b)]. It is important that the interaction between modulated REB and PC provides good mode selection due to effective excitation of only one photonic crystal eigenmode, whose configuration best matches the REB cross-sectional profile. The described mechanism provides the (i) narrow output radiation spectrum, (ii) well focused electromagnetic energy flow in the system, and (iii) high efficiency of distributed electromagnetic feedback via the excited backward wave. With a further REB current increase up to $I_0 = 3.25$ kA, VC oscillation frequency drastically goes beyond area III (≈6.25 GHz) that leads to an interruption of PC high-order mode excitation [Fig. 3(c)]. The frequency of ≈4.5 GHz corresponding to the high-order mode from area II (green point in Fig. 2) is also excited at an average power level in the second and third cases [see Figs. 3(b) and 3(c)] when $I_0 > 2.4$ kA.

Finally, let us consider the impact of the PC structure on the power level and efficiency of microwave generation of the proposed vircator scheme in dependency on beam current I_0. Here, we estimate generation efficiency as $\eta = P_{out}/(I_0 U_0)$. The corresponding plots are shown in Fig. 4. We have calculated output power by integration of the longitudinal component of Poynting vector over the transversal cross-

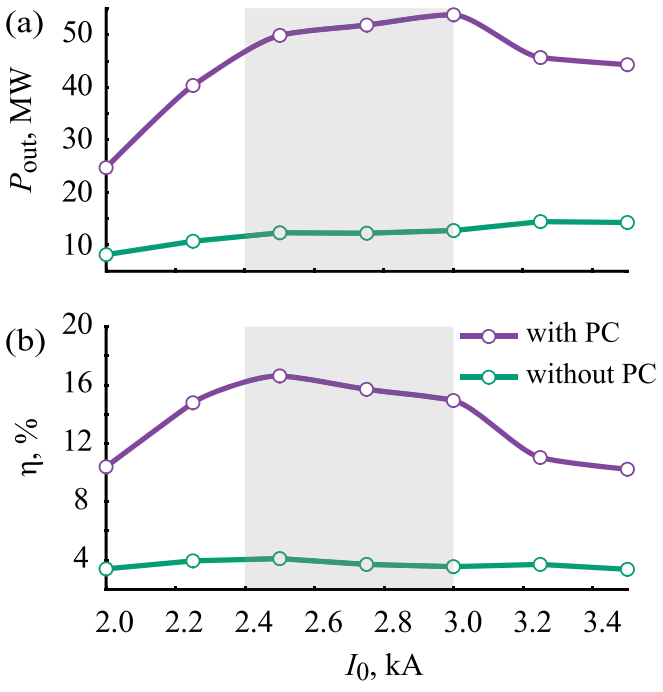

FIG. 4. The dependencies of microwave generation power (a) and efficiency (b) of the virtual cathode oscillator with the photonic crystal (purple curve with circles) and without the photonic crystal (green curve with circles) on beam current I_0. The area highlighted with gray square corresponds to the most effective excitation of photonic crystal eigenwaves by virtual cathode oscillations and the modulated passing beam.

section of the drift tube at the open boundary. Here, we compare the obtained results with the ones calculated for the classical axial vircator without PC to demonstrate the efficiency gain. In this context, two factors worth notation. First, comparison shows that the value of output power as well as generation efficiency considerably increases in the case of PC application. The gain of efficiency reaches 5%–12%, whereas output power gains 2–5 times. Second, one can see that output power and efficiency of the vircator with PC depend nonlinearly on the beam current I_0 in contradistinction to the classical vircator scheme. Thereby, there exists an optimal operation regime of the considered vircator with PC (optimal range of I_0 is highlighted in gray in Fig. 4). In this range of I_0, both output power and generation efficiency attain their maximal values instead of areas of low and high beam currents.

In conclusion, we have shown that PC located in the drift tube of the axial vircator permits us to significantly improve the efficiency of microwave generation due to a number of factors: (i) high interaction impedance with passing REB, (ii) distributed electromagnetic feedback with VC, and (iii) efficient electromagnetic energy output compared to the traditional cylindrical waveguide. Summarizing the above-mentioned facts, one can consider VCO with the photonic crystal as the effective microwave device where the vircator operation mechanism and PC band properties complement each other to produce high-power electromagnetic radiation.

Concerning the experimental realization of the proposed concept, we would like to note several important points. First, one should take into account that the creation of a large magnetic field lowers the total efficiency of the device due to additional energy consumption. However, it can be minimized by optimization of magnetic system parameters. Second, at large values of beam energy and current, one can face the typical problem of HPM, where the high-energy intense beam interacts with the electrodynamical structure—overheating of its elements. In the considered system, one of the ways to avoid this problem is using thicker metal foils (up to 0.7–1.5 mm). In this case, heating is not critical and, at the same time, dispersion properties of PC are conserved.

We are thankful to Professor V. G. Baryshevsky, Dr. A. A. Gurinovich, and Dr. P. V. Molchanov for useful discussions during this research. N.S.F. acknowledges individual financial support from the Russian Foundation for Basic Research (Grant No. 16-32-60107). A.E.H. acknowledges individual financial support from the Ministry of Education and Science of the Russian Federation (Project No. 3.4593.2017/6.7). The works related to the development of the mathematical and numerical models of VCO with PC were supported by the Ministry of Education and Science of the Russian Federation (Project No. 3.859.2017/4.6). The properties of the PC in the VCO scheme were studied with the support of the President's Program (Project No. MK-1163.2017.2). The processes occurring during the interaction of REB with PC in the VCO scheme were studied with the support of the Russian Foundation for Basic Research (Grant No. 17-52-04097). Issues related to the experimental implementation of the proposed scheme were analyzed with the support of the Ministry of Education and Science of the Russian Federation (Project No. 3.6723.2017/8.9).

[1]R. B. Miller, *An Introduction to the Physics of Intense Charged Particle Beams* (Plenum Press, New York, 1982).
[2]V. L. Granatstein and A. V. Gaponov-Grekhov, *Applications of High-Power Microwaves* (Artech House Publishers, 1994).
[3]G. S. Nusinovich and S. H. Gold, "Review of high-power microwave source research," Rev. Sci. Instrum. **68**, 3945–3974 (1997).
[4]A. E. Dubinov, Y. I. Kornilova, and V. D. Selemir, "Collective ion acceleration in systems with a virtual cathode," Phys.-Usp. **45**, 1109–1129 (2002).
[5]R. J. Barker, J. H. Booske, N. C. Luhmann, and G. S. Nusinovich, *Modern Microwave and Millimeter-Wave Power Electronics* (Wiley, New York, 2005).
[6]J. Benford, "Space applications of high-power microwaves," IEEE Trans. Plasma Sci. **36**, 569–581 (2008).
[7]J. Benford, J. A. Swegle, and E. Schamiloglu, *High Power Microwaves*, Series in Plasma Physics, 3rd ed. (CRC Press, Taylor and Francis Group, 2016).
[8]R. A. Mahaffey, P. A. Sprangle, J. Golden, and C. A. Kapetanakos, "High-power microwaves from a non-isochronous reflecting electron system," Phys. Rev. Lett. **39**, 843 (1977).
[9]A. N. Didenko, Y. Krasik, S. P. Perelugin, and G. P. Fomenko, "Generation of power microwave radiation of relativistic beam in triode system," Tech. Phys. Lett. **5**, 321 (1979).
[10]S. C. Burkhart, R. D. Scarpetty, and R. L. Lundberg, "A virtual cathode reflex triode for high power microwave generation," J. Appl. Phys. **58**, 28 (1985).
[11]A. E. Hramov, S. A. Kurkin, A. A. Koronovskii, and A. E. Filatova, "Effect of self-magnetic fields on the nonlinear dynamics of relativistic electron beam with virtual cathode," Phys. Plasmas **19**, 112101 (2012).
[12]D. J. Sullivan, J. E. Walsh, and E. A. Coutsias, "Virtual cathode oscillator (vircator) theory," in *High Power Microwave Sources*, edited by V. L. Granatstein and I. alexeff (Artech House Microwave Library, 1987), Vol. 13.
[13]V. L. Granatstein and I. Alexeeff, *High Power Microwave Sources* (Artech House Microwave Library, 1987).
[14]A. E. Dubinov and V. D. Selemir, "Electronic devices with virtual cathodes (review)," J. Commun. Technol. Electron. **47**, 575 (2002).
[15]S. A. Kurkin, A. A. Badarin, A. K. Alexey, and E. H. Alexander, "Higher harmonics generation in relativistic electron beam with virtual cathode," Phys. Plasmas **21**, 093105 (2014).
[16]S. A. Kurkin, N. S. Frolov, A. O. Rak, A. A. Koronovskii, A. A. Kurayev, and A. E. Hramov, "High-power microwave amplifier based on overcritical relativistic electron beam without external magnetic field," Appl. Phys. Lett. **106**, 153503 (2015).
[17]S. A. Kitsanov, A. I. Klimov, S. D. Korovin, I. K. Kurkan, I. V. Pegel, and S. D. Polevin, "A vircator with electron beam premodulation based on high-current repetitively pulsed accelerator," IEEE Trans. Plasma Sci. **30**, 274–285 (2002).
[18]L. Zhi-Qiang, Z. Hui-Huang, F. Yu-Wei, S. Ting, Y. Jian-Hua, Y. Cheng-Wei, X. Liu-Rong, and Z. Yan-Song, "Simulation and experimental research of a novel vircator," Chin. Phys. Lett. **25**, 2566 (2008).
[19]A. S. Shlapakovski, T. Queller, Y. P. Bliokh, and Y. E. Krasik, "Investigations of a double-gap vircator at sub-microsecond pulse durations," IEEE Trans. Plasma Sci. **40**, 1607–1617 (2012).
[20]S. A. Kurkin, A. E. Hramov, and A. A. Koronovskii, "Microwave radiation power of relativistic electron beam with virtual cathode in the external magnetic field," Appl. Phys. Lett. **103**, 043507 (2013).
[21]M. V. Fazio, J. Kinross-Wright, B. Haynes, and R. F. Hoeberling, "The virtual cathode microwave amplifier experiment," J. Appl. Phys. **66**, 2675–2677 (1989).
[22]N. S. Phrolov, A. A. Koronovskii, Y. A. Kalinin, S. A. Kurkin, and A. E. Hramov, "The effect of an external signal on output microwave power of a low-voltage vircator," Phys. Lett. A. **378**, 2423–2428 (2014).
[23]R. Platt, B. Anderson, J. Christofferson, J. Enns, M. Haworth, J. Metz, P. Pelletler, R. Rupp, and D. Voss, "Low-frequency, multigigawatt microwave pulses generated by a virtual cathode oscillator," Appl. Phys. Lett. **54**, 1215 (1989).
[24]S. A. Kurkin and A. E. Hramov, "Virtual cathode formation in annular electron beam in an external magnetic field," Tech. Phys. Lett. **35**, 23–25 (2009).

[25]S. A. Kurkin, A. A. Badarin, A. A. Koronovskii, and A. E. Hramov, "The development and interaction of instabilities in intense relativistic electron beams," Phys. Plasmas **22**, 122110 (2015).
[26]W. Jiang and M. Kristiansen, "Theory of the virtual cathode oscillator," Phys. Plasmas **8**, 3781–3787 (2001).
[27]S. A. Kurkin, A. A. Koronovskii, and A. E. Hramov, "Output microwave radiation power of low-voltage vircator with external inhomogeneous magnetic field," Tech. Phys. Lett. **37**, 356–359 (2011).
[28]W. Jiang, J. Dickens, and M. Kristiansen, "Efficiency enhancement of a coaxial virtual cathode oscillator," IEEE Trans. Plasma Sci. **27**, 1543–1544 (1999).
[29]A. E. Dubinov, I. A. Efimova, K. E. Mikheev, V. D. Selemir, and V. P. Tarakanov, "Hybrid microwave oscillators with a virtual cathode," Plasma Phys. Rep. **30**, 496 (2004).
[30]Y.-W. Fan, H.-H. Zhong, Z.-Q. Li, T. Shu, J.-D. Zhang, J. Zhang, X.-P. Zhang, J.-H. Yang, and L. Luo, "A double-band high-power microwave source," J. Appl. Phys. **102**, 103304 (2007).
[31]S. Champeaux, P. Gouard, R. Cousin, and J. Larour, "3-d pic numerical investigations of a novel concept of multistage axial vircator for enhanced microwave generation," IEEE Trans. Plasma Sci. **43**, 3841–3855 (2015).
[32]N. S. Frolov, S. A. Kurkin, A. A. Koronovskii, and A. E. Hramov, "Nonlinear dynamics and bifurcation mechanisms in intense electron beam with virtual cathode," Phys. Lett. A **381**, 2250–2255 (2017).
[33]N. N. Gadetskii, I. I. Magda, S. I. Naisteter, Y. V. Prokopenko, and V. I. Tchumakov, "The virtode: A generator using supercritical REB current with controlled feedback," Plasma Phys. Rep. **19**, 273 (1993).
[34]C. M. Soukoulis, *Photonic Band Gap Materials* (Springer Netherlands, 1996).
[35]K. Yasumoto, *Electromagnetic Theory and Applications for Photonic Crystals* (CRC Press, 2005).
[36]V. Baryshevsky, "Spontaneous and induced radiation by electrons/positrons in natural and photonic crystals. volume free electron lasers (VFELs): From microwave and optical to x-ray range," Nucl. Instrum. Methods Phys. Res., Sect. B **355**, 17–23 (2015).
[37]B. Wang and M. A. Cappelli, "A plasma photonic crystal bandgap device," Appl. Phys. Lett. **108**, 161101 (2016).
[38]V. S. Babitski, V. G. Baryshevsky, A. A. Gurinovich, E. A. Gurnevich, P. V. Molchanov, L. V. Simonchik, M. S. Usachonak, and R. F. Zuyeuski, "Delay of a microwave pulse in a photonic crystal," J. Appl. Phys. **122**, 083104 (2017).
[39]V. G. Baryshevsky and A. A. Gurinovich, "Hybrid systems with virtual cathode for high power microwaves generation," preprint arXiv:0903.0300 (2009).
[40]V. G. Baryshevsky, N. A. Belous, A. A. Gurinovich, E. A. Gurnevich, V. A. Evdokimov, and P. V. Molchanov, "Experimental studies of volume FELS with a photonic crystal made of foils," in Proceedings of FEL2010 (2010).